24th INTERNATIONAL CONGRESS ON SOUND AND VIBRATION
23–27 July 2017, London

NONLINEAR FREE VIBRATION OF SHEAR DEFORMABLE FUNCTIONALLY GRADED POROUS BEAMS

Jie Yang

School of Engineering, RMIT University, PO Box 71, Bundoora, VIC 3083, Australia
email: j.yang@rmit.edu.au

Da Chen, Sritawat Kitipornchai

School of Civil Engineering, the University of Queensland, St Lucia, Brisbane, QLD 4072, Australia
email: d.chen@uq.edu.au; s.kitipornchai@uq.edu.au

This paper presents a nonlinear free vibration analysis of functionally graded (FG) porous beams with non-uniform porosity distributions. Timoshenko beam theory is employed to take into account the effect of transverse shear strains. The elastic moduli and mass density of porous beams vary continuously along the thickness direction based on symmetric and asymmetric porosity distributions. The typical mechanical property of an open-cell metal foam is used to obtain the relationship between coefficients of porosity and mass density. Based on von Kármán type nonlinear strain-displacement relationships, the governing equation is derived with Ritz method and solved by a direct iterative algorithm. The effects of varying porosity distributions, porosity coefficients, boundary conditions and slenderness ratios are investigated through a detailed parametric study, indicating an effective way to improve the vibration behaviour of porous beams.

Keywords: functionally graded porous beam; nonlinear free vibration; Timoshenko beam theory; Ritz method.

1. Introduction

Functionally graded materials (FGMs) are newly developed with material properties varying continuously and smoothly along one or more directions, offering unique advantages compared to conventional homogeneous materials, such as the freedom to tailor local properties to meet special design requirements. Porous structure is another novel structural form that has attracted increasing attention from research and engineering communities [1]. It introduces the mass density as a new design parameter, and is considered to be a perfect candidate for lightweight structures. As a typical form of porous structures, metal foams also present great potential in impact engineering with excellent energy absorption capacities [2, 3].

Structures with graded porosity, i.e., FG porous structures, can be considered as the combination of FGMs and porous structures, which enable non-uniform distributions of internal pores and provide novel structural properties. The research of FG porous structures is still in the very early stage, with most of current studies focusing on the static deformation and stability problems. Magnucka-Blandzi [4] conducted the nonlinear analysis of dynamic stability of FG metal foam circular plate under radial compression. She [5] also proposed the mathematical modelling of a simply supported rectangular sandwich plate consisting of two isotropic facings and an FG metal foam core. Chen et al. [6] presented the elastic buckling and static bending solutions for porous beams with graded porosity distributions.

The vibration behaviour of FG structures is crucial for their applications and needs to be well understood. Fallah and Aghdam [7] derived simple analytical expressions for large amplitude free vibration and postbuckling analyses of FG beams on nonlinear elastic foundations. Rafiee et al. [8] applied a temperature change and a voltage to an FG composite beam reinforced by carbon nanotubes and bonded by piezoelectric layers, and studied its large amplitude vibrations. Kitipornchai et al. [9] proposed a semi-analytical solution for the nonlinear vibration of shear deformable laminated rectangular plate consisting of a homogeneous core and two FG face layers, and evaluated the influence of geometric imperfections. The nonlinear vibration behaviour of FG shells has been studied by Loy et al. [10], Strozzi and Pellicano [11] and Pradhan et al. [12], among many others.

This paper investigates the nonlinear free vibration behaviour of shear deformable FG porous beams within the framework of Timoshenko beam theory. Three typical boundary conditions are employed, including hinged-hinged (H-H), clamped-clamped (C-C), and clamped-hinged (C-H) end supports. Ritz method and a direct iterative algorithm are used to obtain the nonlinear frequency ratios of porous beams with two non-uniform porosity distributions. A detailed parametric study is conducted to shed important insights into the design of porous structures with enhanced dynamic performance.

2. Functionally graded porous beams

The porosity distributions of functionally graded porous beams are assumed to vary nonlinearly along the thickness direction. Two distributions are considered in this paper, i.e., symmetric distribution (porosity distribution 1) and asymmetric distribution (porosity distribution 2), as shown in Fig. 1. As can be observed, the size and density of internal pores reach the maximum values at the mid-plane of the beam with porosity distribution 1, while on the bottom surface of the beam with distribution 2, corresponding to the minimum values of elastic moduli and mass density.

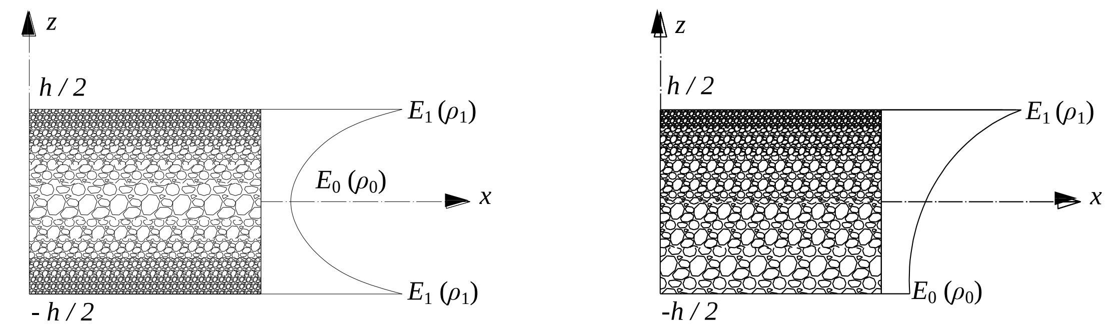

(a) Porosity distribution 1 (symmetric) (b) Porosity distribution 2 (asymmetric)

Figure 1: Two non-uniform porosity distributions.

Due to the graded porosity distributions, Young modulus, shear modulus and mass density of porous beams are position-dependent and can be calculated from Eq. (1) for porosity distribution 1 and Eq. (2) for porosity distribution 2.

$$\begin{cases} E(z) = E_1\left[1 - e_0 \cos\left(\pi \dfrac{z}{h}\right)\right] \\ G(z) = G_1\left[1 - e_0 \cos\left(\pi \dfrac{z}{h}\right)\right] \\ \rho(z) = \rho_1\left[1 - e_m \cos\left(\pi \dfrac{z}{h}\right)\right] \end{cases} \tag{1}$$

$$\begin{cases} E(z)=E_1\left[1-e_0\cos\left(\dfrac{\pi}{2}\dfrac{z}{h}+\dfrac{\pi}{4}\right)\right] \\ G(z)=G_1\left[1-e_0\cos\left(\dfrac{\pi}{2}\dfrac{z}{h}+\dfrac{\pi}{4}\right)\right] \\ \rho(z)=\rho_1\left[1-e_m\cos\left(\dfrac{\pi}{2}\dfrac{z}{h}+\dfrac{\pi}{4}\right)\right] \end{cases} \tag{2}$$

where *z*-axis is along the thickness direction and *x*-axis is along the length direction, *h* is the beam thickness, E_1 (G_1, ρ_1) is the maximum value of Young modulus (shear modulus, mass density), E_0 (G_0, ρ_0) is the corresponding minimum value, and

$$G_i=\frac{E_i}{2(1+v)} \quad (i=0,1) \tag{3}$$

in which *v* is Poisson's ratio which is taken as a constant. The porosity coefficient e_0 and density coefficient e_m are calculated by

$$\begin{cases} e_0=1-\dfrac{E_0}{E_1}=1-\dfrac{G_0}{G_1} \\ e_m=1-\dfrac{\rho_0}{\rho_1} \end{cases} \tag{4}$$

and can be related by Eq. (5) using the typical mechanical property in Eq. (6) of an open-cell metal foam [6]. It should be noted that E_1, G_1 and ρ_1 also correspond to the material parameters of beams without internal pores.

$$e_m=1-\sqrt{1-e_0} \tag{5}$$

$$\frac{E_0}{E_1}=\left(\frac{\rho_0}{\rho_1}\right)^2 \tag{6}$$

3. Theoretical formulations

Timoshenko beam theory is employed in this paper to consider the effect of transverse shear strains. The associated displacement fields are

$$\begin{cases} u_x(x,z,t)=u_0(x,t)+z\phi_x(x,t) \\ w_z(x,z,t)=w_0(x,t) \end{cases} \tag{7}$$

where u_0 and w_0 are the axial and transverse displacements on the mid-plane of the beam, ϕ_x is the rotation of the beam cross section, and *t* denotes time. To include von Kármán geometric nonlinearity, the strain-displacement relationships are given as [13]

$$\begin{cases} \varepsilon_{xx}=\dfrac{\partial u_0}{\partial x}+z\dfrac{\partial \phi_x}{\partial x}+\dfrac{1}{2}\left(\dfrac{\partial w_0}{\partial x}\right)^2 \\ \gamma_{xz}=\dfrac{\partial w_0}{\partial x}+\phi_x \end{cases} \tag{8}$$

where ε_{xx} and γ_{xz} are the normal and transverse shear strains, and can be used to obtain the corresponding stresses through the elastic constitutive law as

$$\begin{cases} \sigma_{xx} = \dfrac{E(z)}{1-v^2}\varepsilon_{xx} \\ \tau_{xz} = G(z)\gamma_{xz} \end{cases} \tag{9}$$

The strain energy U and kinetic energy K of the porous beam can be written as

$$U = \frac{1}{2}\int_0^L \left\{ A_{11}\left[\frac{\partial u_0}{\partial x} + \frac{1}{2}\left(\frac{\partial w_0}{\partial x}\right)^2\right]^2 + 2B_{11}\left[\frac{\partial \phi_x}{\partial x}\frac{\partial u_0}{\partial x} + \frac{1}{2}\frac{\partial \phi_x}{\partial x}\left(\frac{\partial w_0}{\partial x}\right)^2\right] + D_{11}\left(\frac{\partial \phi_x}{\partial x}\right)^2 + A_{55}\left(\phi_x + \frac{\partial w_0}{\partial x}\right)^2 \right\} dx \tag{10}$$

$$K = \frac{1}{2}\int_0^L \left\{ I_0\left[\left(\frac{\partial u_0}{\partial t}\right)^2 + \left(\frac{\partial w_0}{\partial t}\right)^2\right] + 2I_1\frac{\partial \phi_x}{\partial t}\frac{\partial u_0}{\partial t} + I_2\left(\frac{\partial \phi_x}{\partial t}\right)^2 \right\} dx \tag{11}$$

where L is the beam length, and the stiffness components and inertia items are defined by

$$\begin{cases} \{A_{11}, B_{11}, D_{11}\} = \displaystyle\int_{-h/2}^{h/2} \frac{E(z)}{1-v^2}\left\{1, z, z^2\right\} \mathrm{d}z \\ A_{55} = \displaystyle\int_{-h/2}^{h/2} kG(z)\mathrm{d}z \end{cases} \tag{12}$$

$$\{I_0, I_1, I_2\} = \int_{-h/2}^{h/2} \rho(z)\left\{1, z, z^2\right\} \mathrm{d}z \tag{13}$$

of which $k = 5/6$ is the shear correction factor.

Assuming that the proposed beam undergoes harmonic vibrations, the following nonlinear governing equation can be derived based on Ritz method.

$$(\mathbf{K}_\mathrm{l} + \mathbf{K}_\mathrm{nl} - \omega^2\mathbf{M})\mathbf{d}_0 = 0 \tag{14}$$

where $\mathbf{K}_\mathrm{l}$ is the linear stiffness matrix, $\mathbf{K}_\mathrm{nl}$ is the nonlinear stiffness matrix, ω is the natural frequency of the beam, $\mathbf{M}$ is the mass matrix, the unknown coefficient vector $\mathbf{d}_0$ is given as

$$\mathbf{d}_0 = \{\{R_{1j}\}^\mathrm{T}\{R_{2j}\}^\mathrm{T}\{R_{3j}\}^\mathrm{T}\}^\mathrm{T} \tag{15}$$

where R_{1j} , R_{2j} , R_{3j} ($j = 1, 2, \cdots, N$) are the unknown coefficients in Ritz trial functions [6], and N is the total number of polynomial terms. A direct iterative algorithm [13] is employed to obtain the nonlinear frequency ω_nl and the nonlinear frequency ratio $\omega_\mathrm{nl}/\omega_\mathrm{l}$ (ω_l is the linear fundamental frequency) of porous beams.

4. Numerical results

A detailed parametric study is carried out to investigate the influences of porosity distribution, porosity coefficient, boundary condition and slenderness ratio on the nonlinear vibration behavior of porous beams composed of open-cell steel foam with $E_1 = 200\,\mathrm{GPa}$, $v = 1/3$, $\rho_1 = 7850$ kg/m^3. The total number of polynomial terms in Ritz trial functions is taken as $N = 10$ to ensure the convergence of results. Table 1 gives the nonlinear frequency ratios of functionally graded (FG-) and uniformly distributed (UD-) carbon nanotube-reinforced composite (CNTRC) beams with different boundary conditions. W_{max} is the given positive vibration amplitude. Our results are in excellent agreement with those obtained by Ke et al. [13] from which the material parameters of CNTRC beams, which are not given here for brevity, can be found.

Table 1: Nonlinear frequency ratio of FG- and UD-CNTRC beams ($V_{cnt}^{*} = 0.17$, $L/h = 10$)

	FG-CNTRC beam		UD-CNTRC beam	
	Present	Ke et al. [13]	Present	Ke et al. [13]
W_{max}	H-H beam			
0.1	1.0046	1.0046	1.0261	1.0259
0.2	1.0256	1.0255	1.1006	1.1000
0.3	1.0758	1.0765	1.2148	1.2135
	C-C beam			
0.1	1.0148	1.0146	1.0137	1.0136
0.2	1.0581	1.0574	1.0540	1.0533
0.3	1.1265	1.1252	1.1177	1.1165
	C-H beam			
0.1	1.0144	1.0139	1.0190	1.0187
0.2	1.0566	1.0554	1.0738	1.0727
0.3	1.1253	1.1243	1.1586	1.1570

Fig. 2(a) and Fig. 2(b) present the effect of porosity coefficient on the nonlinear frequency ratio versus vibration amplitude curves for H-H FG porous beams with different porosity distributions. Results show that an increase in the vibration amplitude leads to a larger ratio, thus a higher nonlinear frequency. For symmetric porosity distribution 1, the nonlinear frequency ratio decreases with the increasing of porosity coefficient. While for asymmetric distribution 2, as the porosity coefficient increases, the nonlinear frequency ratio varies slightly under positive vibration amplitude W_{max}, but decreases dramatically under negative amplitude W_{min}. This is caused by the bending-extension coupling effect within the asymmetric material distribution, leading to different vibration amplitudes at positive and negative half cycles.

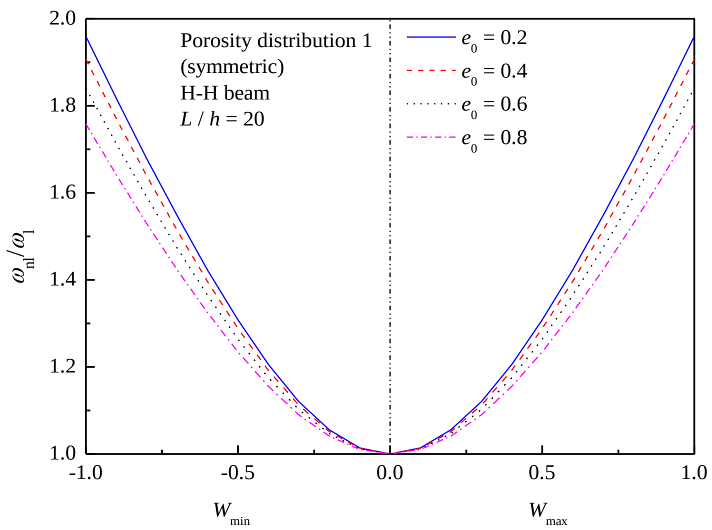

(a) Porosity distribution 1

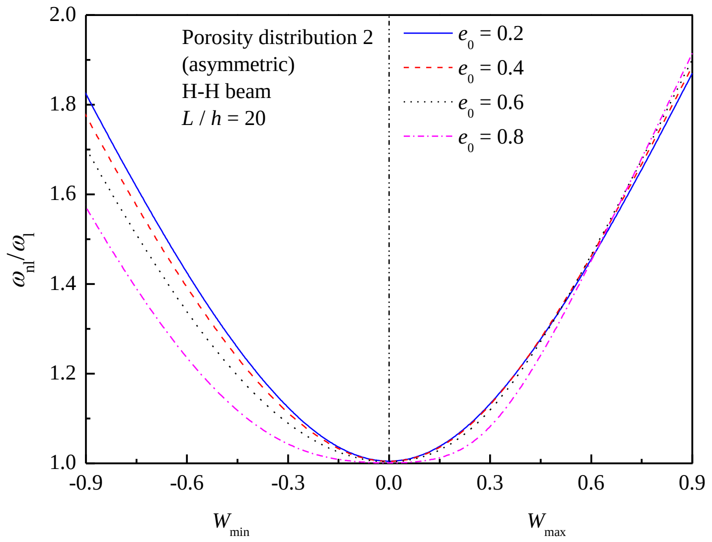

(b) Porosity distribution 2

Figure 2: Nonlinear frequency ratio versus vibration amplitude curves for H-H FG porous beams: effect of porosity coefficient.

Fig. 3(a) and Fig. 3(b) compare the nonlinear frequency ratios and dimensionless nonlinear frequencies of FG porous beams with varying porosity distributions and boundary conditions, respectively. The dimensionless nonlinear frequency is calculated as

$$\omega_{nl}^{*} = \omega_{nl} L \sqrt{\frac{I_{10}}{A_{110}}} \tag{16}$$

where I_{10} and A_{110} are the values of I_0 and A_{11} of homogeneous materials without pores. It can be seen that the nonlinear frequency ratio of beams with symmetric porosity distribution 1 is always smaller than that of beams with asymmetric distribution 2. Due to relatively high linear fundamental frequency, however, the nonlinear frequency of beams with distribution 1 is larger, indicating higher effective beam stiffness. Also, as expected, C-C beams have the highest nonlinear frequencies, thus the best vibration resistance.

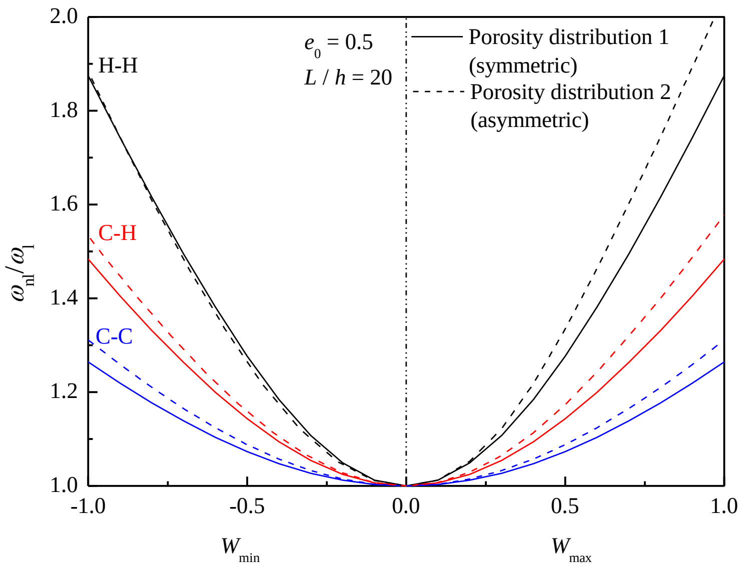

(a) Nonlinear frequency ratio versus vibration amplitude

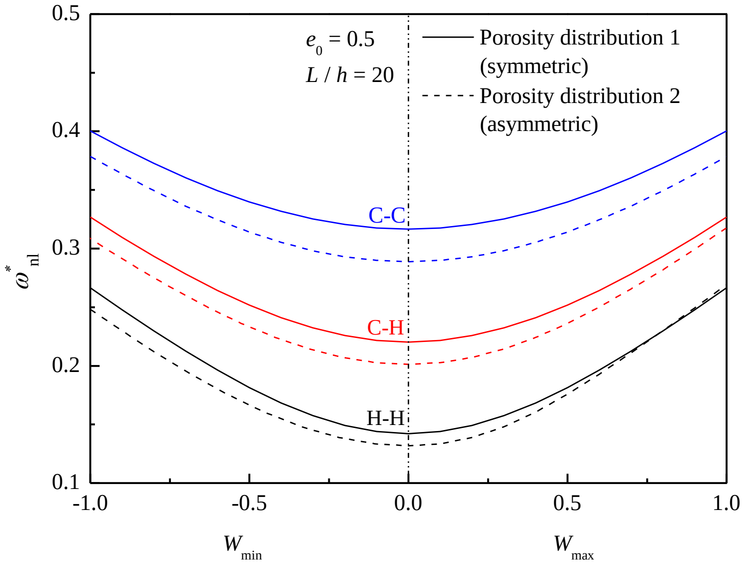

(b) Nonlinear frequency versus vibration amplitude

Figure 3: Comparisons of nonlinear frequency ratios and dimensionless nonlinear frequencies of FG porous beams with varying porosity distributions and boundary conditions.

Table 2 tabulates the nonlinear frequency ratios of FG porous beams with different slenderness ratios. It can be found that although decreases the linear fundamental frequency dramatically, an increase in the slenderness ratio only brings slight decrease of nonlinear frequency ratio.

Table 2: Nonlinear frequency ratio of FG porous beams: effect of slenderness ratio ($e_0 = 0.5$)

	Porosity distribution 1			Porosity distribution 2		
	$L/h=20$	$L/h=30$	$L/h=40$	$L/h=20$	$L/h=30$	$L/h=40$
W_{max}	H-H beam					
0.2	1.0492	1.0490	1.0489	1.0527	1.0524	1.0523
0.4	1.1843	1.1835	1.1833	1.2184	1.2175	1.2172
0.6	1.3810	1.3795	1.3789	1.4631	1.4619	1.4613
	C-C beam					
0.2	1.0121	1.0120	1.0120	1.0147	1.0145	1.0145
0.4	1.0476	1.0471	1.0469	1.0571	1.0567	1.0565
0.6	1.1036	1.1029	1.1025	1.1237	1.1228	1.1225
	C-H beam					
0.2	1.0245	1.0243	1.0243	1.0290	1.0288	1.0288
0.4	1.0939	1.0933	1.0931	1.1136	1.1129	1.1126
0.6	1.1996	1.1984	1.1980	1.2427	1.2416	1.2412

5. Conclusions

The nonlinear free vibration behavior of shear deformable FG porous beams has been investigated within the framework of Timoshenko beam theory and von Kármán geometric nonlinearity. The effects of varying parameters are discussed in detail. It can be concluded that an increased porosity coefficient decreases the nonlinear frequency ratio of porous beams. Compared with the non-uniform asymmetric porosity distribution (distribution 2), the non-uniform symmetric porosity distribution (distribution 1) offers larger nonlinear frequency, thus higher effective beam stiffness and improved vibration behavior. Also, fully clamped end supports can provide the best vibration resistance, and the slenderness ratio actually has no evident influence on the nonlinear frequency ratio of porous beams.

ACKNOWLEDGEMENTS

The work described in this paper was fully funded by an Australian Government Research Training Program Scholarship and research grants from the Australian Research Council under Discovery Project scheme (DP140102132, DP160101978, LP150100103, LP150101033). The authors are grateful for their financial support.

REFERENCES

1 Gibson, L.J. and Ashby, M.F., *Cellular Solids: Structure and Properties*, Cambridge University Press, Cambridge, UK, (1997).

2 Ashby, M.F., Evans, T., Fleck, N.A., Hutchinson, J., Wadley, H. and Gibson, L., *Metal Foams: A Design Guide*, Butterworth-Heinemann, Boston, USA, (2000).

3 Pinnoji, P.K., Mahajan, P., Bourdet, N., Deck, C. and Willinger, R.m. Impact Dynamics of Metal Foam Shells for Motorcycle Helmets: Experiments & Numerical Modeling, *International Journal of Impact Engineering*, **37**, 274-284, (2010).

4 Magnucka-Blandzi, E. Non-Linear Analysis of Dynamic Stability of Metal Foam Circular Plate, *Journal of Theoretical and Applied Mechanics*, **48**, 207-217, (2010).

5 Magnucka-Blandzi, E. Mathematical Modelling of a Rectangular Sandwich Plate with a Metal Foam Core, *Journal of Theoretical and Applied Mechanics*, **49**, 439-455, (2011).

6 Chen, D., Yang, J. and Kitipornchai, S. Elastic Buckling and Static Bending of Shear Deformable Functionally Graded Porous Beam, *Composite Structures*, **133**, 54-61, (2015).

7 Fallah, A. and Aghdam, M. Nonlinear Free Vibration and Post-Buckling Analysis of Functionally Graded Beams on Nonlinear Elastic Foundation, *European Journal of Mechanics-A/Solids*, **30**, 571-583, (2011).

8 Rafiee, M., Yang, J. and Kitipornchai, S. Large Amplitude Vibration of Carbon Nanotube Reinforced Functionally Graded Composite Beams with Piezoelectric Layers, *Composite Structures*, **96**, 716-725, (2013).

9 Kitipornchai, S., Yang, J. and Liew, K. Semi-Analytical Solution for Nonlinear Vibration of Laminated Fgm Plates with Geometric Imperfections, *International Journal of Solids and Structures*, **41**, 2235-2257, (2004).

10. Loy, C.T., Lam, K.Y. and Reddy, J.N. Vibration of Functionally Graded Cylindrical Shells, *International Journal of Mechanical Sciences*, **41**, 309-324, (1999).

11. Strozzi, M. and Pellicano, F., Nonlinear Vibrations of FGM Circular Cylindrical Shells, *Thin-Walled Structures*, **67**, 63-77, (2013).

12. Pradhan, S.C., Loy, C.T., Lam, K.Y. and Reddy, J.N. Vibration characteristics of functionally graded cylindrical shells under various boundary conditions, *Applied Acoustics*, **61**, 111-29, (2000).

13 Ke, L.-L., Yang, J. and Kitipornchai, S. Nonlinear Free Vibration of Functionally Graded Carbon Nanotube-Reinforced Composite Beams, *Composite Structures*, **92**, 676-683, (2010).